

Thermally induced switching field distribution of a single CoPt dot in a large array

J B C Engelen¹, M Delalande¹, A J le Fèvre¹, T Bolhuis¹,
T Shimatsu², N Kikuchi², L Abelmann¹ and J C Lodder¹

¹ MESA⁺ Institute for Nanotechnology, University of Twente, Enschede, The Netherlands

² Tohoku University, Sendai, Japan

E-mail: l.abelmann@utwente.nl

Received 22 October 2009, in final form 19 November 2009

Published 7 December 2009

Online at stacks.iop.org/Nano/21/035703

Abstract

Magnetic dot arrays with perpendicular magnetic anisotropy were fabricated by patterning Co₈₀Pt₂₀-alloy continuous films by means of laser interference lithography. As commonly seen in large dot arrays, there is a large difference in the switching field between dots. Here we investigate the origin of this large switching field distribution, by using the anomalous Hall effect (AHE). The high sensitivity of the AHE permits us to measure the magnetic reversal of individual dots in an array of 80 dots with a diameter of 180 nm. By taking 1000 hysteresis loops we reveal the thermally induced switching field distribution SFD_T of individual dots inside the array. The SFD_T of the first and last switching dots were fitted to an Arrhenius model, and a clear difference in switching volume and magnetic anisotropy was observed between dots switching at low and high fields.

(Some figures in this article are in colour only in the electronic version)

1. Introduction

To continue the areal density growth in magnetic recording beyond the limits set by thermal fluctuations, bit patterned media are required in which each bit is a single domain nanomagnetic dot. An important parameter of patterned media is the switching field distribution (SFD) of the array of dots. In order to achieve error-free writing in high density magnetic data storage, it is important for all dots to reverse magnetization at the same external field. However, experimentally much broader distributions are found than what is expected for such highly exchange coupled systems [1].

In order to understand the origins of these large variations in switching fields in an array, we investigate the switching behavior of individual dots. The switching field of an individual dot varies slightly each time a hysteresis loop is measured. Besides the SFD of the ensemble of dots in the array, the individual dots show a thermally induced SFD (SFD_T). When the SFD_T is measured, it can be used to determine the height and shape of the energy barrier between the two stable magnetic states in the dots.

To measure the reversal of the nanometer sized dots inside the array, a very sensitive magnetometry technique is required. Techniques that are sensitive enough to sense individual dots include μ SQUID operated at cryogenic temperatures [2] and magnetic force microscopy (MFM) [1]. Anomalous Hall effect (AHE) measurements are very sensitive, can be operated in a wide temperature range including room temperature and do not require extensive sample preparation. This method has previously successfully been applied to measure single nanodots [3–5] and dot arrays [3, 4, 6–8]. Detection of the reversal of individual dots inside an array, however, requires a very low noise measurement, and has—to our knowledge—not been reported up to now. In this work, AHE is used for the first time to measure the SFD of a single dot in an array of about 80 Co₈₀Pt₂₀ 180 nm dots. By careful optimization of the setup, it is possible to repeatedly measure the switching of a single dot and determine SFD_T. The results can be used to model the switching behavior of single dots inside the array. Instead of measuring on 80 single dot crosses (only one dot per Hall cross) to obtain information about weak and strong dots, our alternative is to measure on an array of 80 dots

where it is possible to pinpoint the weakest and strongest dots directly and measure their SFD. The method of using AHE measurements on arrays of magnetic dots therefore provides a practical approach to investigate the origins of the SFD in patterned magnetic films.

In the following, we first discuss the experimental preparation and measurement conditions and continue with the results of measurements on the complete array and of single dots within the array. Subsequently the Arrhenius model that was developed to fit to the measurements is discussed and applied to the thermal SFD_T of two dots switching at different fields.

2. Description of sample and AHE measurement

Magnetic polycrystalline Co₈₀Pt₂₀ alloy 20 nm thin films with high perpendicular anisotropy were deposited at room temperature using magnetron co-sputtering on Ru(20 nm)/Pt(10 nm)/Ta(5 nm) buffer layers on a thermally oxidized Si substrate. The structure and magnetic properties of these thin films have been studied in previous works [7, 9]. The hcp-CoPt(002) plane is epitaxially grown on the (002) plane of the Ru buffer layer, and has a full-width angle distribution of 2.8° at half-maximum. TEM analysis revealed that the Co₈₀Pt₂₀ alloy film has a mean grain diameter of 14 nm.

The magnetic easy axis of the film is perpendicular to the film plane with a saturation magnetization M_s and an intrinsic anisotropy constant K_u ($=K_{\text{eff}} + \frac{N}{2}\mu_0 M_s^2$) of 1200 kA m⁻¹ and 1.30×10^6 J m⁻³ respectively, as determined by using a vibrating sample magnetometer and a torque magnetometer.

Laser interference lithography was used to create a dot array etch mask of positive resist [10]. This resist pattern was transferred into the magnetic Co₈₀Pt₂₀ layer by means of ion beam etching. The dot diameter is about 180 nm and the periodicity of the array 600 nm.

When current flows through a material and an external magnetic field is applied, a Hall voltage is generated perpendicular to the current flow and perpendicular to the applied magnetic field; the magnetization of ferromagnetic materials generates an extra Hall voltage, called the anomalous Hall effect (AHE) [11, 12]. For a current in the x direction, the Hall voltage in the y direction will only depend on the external field H and material's magnetization M in the z direction

$$V_y = (\mu_0 H_z R_0 + \mu_0 M_z R_s) \frac{I_x}{t}, \quad (1)$$

where t , R_0 and R_s are the material's thickness, and the normal and anomalous Hall coefficients, respectively. Generally, $R_0 \ll R_s$.

In our AHE measurements, the conducting buffer layers function as electrodes, and are patterned into square Hall crosses. Figure 1 shows a SEM picture of a dot array on top of a 4 μm wide square Hall cross. A portion of the current flowing through the buffer layers also flows through the dots and generates an AHE voltage depending on the magnetization of the dots. The measured Hall voltage V_H is the sum of the

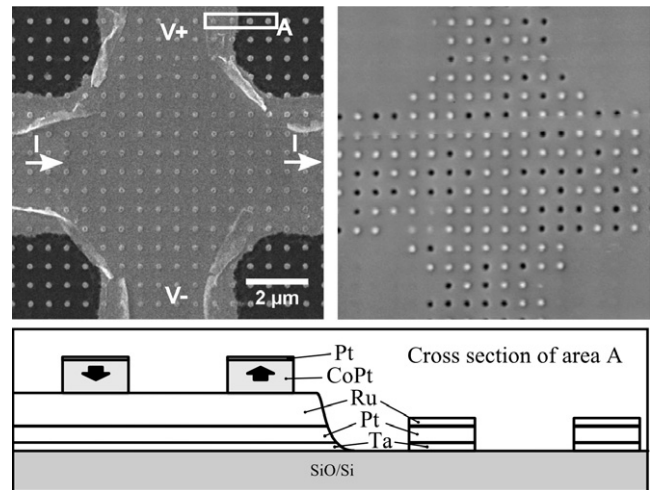


Figure 1. SEM and MFM images of the 4 μm wide Hall cross connecting to the dot array. The central area of the cross covers about 80 dots, which have a mean diameter of 180 nm and thickness of 20 nm. The MFM image shows that only the dots on top of the Hall cross are magnetic.

Hall voltage from the buffer layers V_{buf} and the Hall voltage from the dots, and can be written, to a first approximation, as:

$$V_H = V_{\text{buf}} + \sum_{\text{all dots}} S(x_i, y_i) \cdot V_{\text{dot}}^i, \quad (2)$$

where S is a spatial sensitivity function—maximum in the central area of the cross—similar to the one defined by Webb and Schultz [13], and V_{dot}^i the Hall voltage from dot i at location (x_i, y_i) . The normal Hall coefficient R_0 of the buffer layers and the dots is much smaller than the anomalous Hall coefficient R_s of the dots. Therefore, V_{dot}^i is mainly determined by the perpendicular component M_{\perp} of the dot's magnetization, and the contribution to V_{buf} from the stray field of the dots is very small compared to the voltage from the dots. In the magnetically saturated region, where the Hall contribution of the dots is constant, V_{buf} depends linearly on the applied field H , and can be subtracted from the measurement by fitting a straight line to the measured V_H .

All measurements were done at controlled room temperature and, unless stated otherwise, the magnetic field is applied perpendicular to the Hall cross plane. By carefully optimizing the measurement setup it was possible to measure very close to the theoretical noise limit of the Hall cross. The AHE measurements were carried out using a 1 mA AC current at 833 Hz and a lock-in amplifier with 300 ms integration time; every 3 s a measurement is taken and the external field is increased according to the desired sweep rate.

3. Measurements on a dot array

3.1. Angular dependence of coercivity

In figure 2, AHE voltage curves of a continuous film (a) and a 180 nm dot array (b) are plotted as functions of the applied magnetic field. After patterning, the coercivity increases from 19 to 300 kA m⁻¹, but remains lower than the

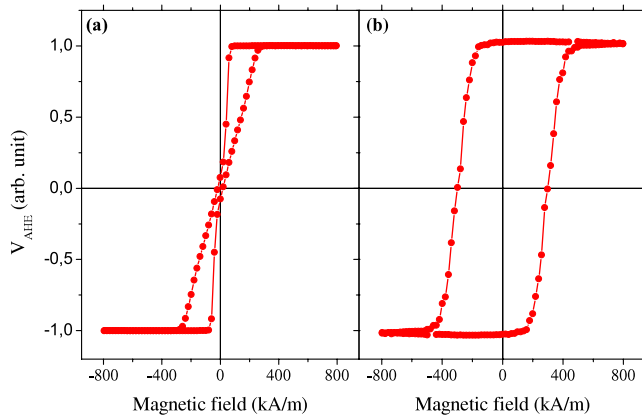


Figure 2. AHE hysteresis curves for (a) continuous film and (b) 180 nm dots array of $\text{Co}_{80}\text{Pt}_{20}$ film (measured at room temperature and for an applied magnetic field perpendicular to the film plane).

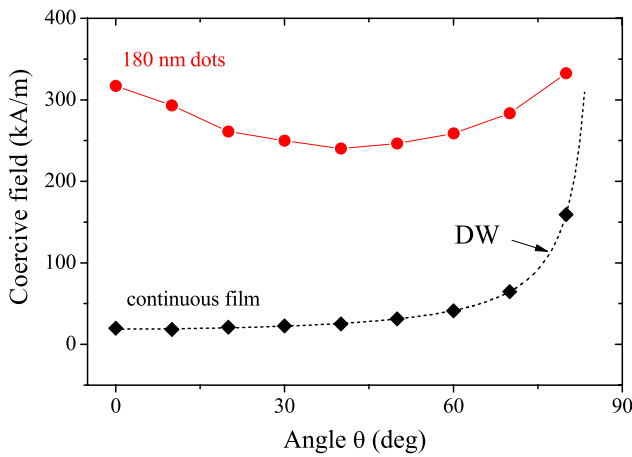


Figure 3. Switching field of continuous film and 180 nm dot array versus the angle θ between the applied field direction and film normal. The dashed line shows the angular dependency as expected for domain wall motion (DW). The solid line is a 'guide to the eye'.

anisotropy field H_k determined from the effective anisotropy constant (540 kA m^{-1}). To obtain more information about the switching mechanism, measurements with different angles for the applied magnetic field have been done by using the AHE measurement method. In figure 3, the measured coercivity H_c is plotted against the angle θ between the applied field direction and film normal. The coercive field³ corresponds to the average switching field of the dot array. For the continuous film, the switching field as a function of applied field angle θ is proportional to $1/\cos\theta$ (dashed line 'DW'), indicating that magnetization reversal is controlled by domain wall motion [14], as expected. After patterning, the 180 nm dots array exhibits a Stoner–Wohlfarth-like angular dependence with a minimum close to 45° . However, deviations from the coherent rotation model are observed since the curve shows an asymmetry which can be reproduced by the modified Kondorsky model in which wall motion and coherent rotation

³ Value of applied field for which the Hall voltage, after correction of the offset and NHE voltage, is zero.

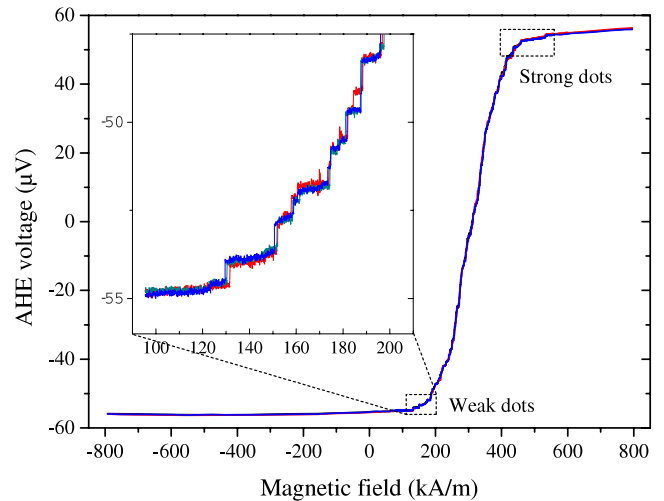


Figure 4. Three overlying AHE curves of the 180 nm $\text{Co}_{80}\text{Pt}_{20}$ dot array. The linear NHE voltage and the DC offset voltage of $520 \mu\text{V}$ have been subtracted from V_H . The step size in magnetic field from 0 to 550 kA m^{-1} is 80 A m^{-1} , resulting in a magnetic field sweep rate R of $50 \text{ A m}^{-1} \text{ s}^{-1}$. The inset shows a magnification of the measurement, clearly showing steps and plateaus, caused by the magnetization reversal of single dots.

are combined [15]. From MFM measurements on a single 180 nm dot, we conclude that a single dot without applied magnetic field has a homogeneous magnetization. Although during switching the magnetization can be non-homogeneous, after switching the dot magnetization is single domain.

3.2. Steps in AHE voltage due to single dots

Figure 4 shows three of 1000 repeated magnetization versus field measurements. The measurements start at negative saturation and were taken at a low magnetic field sweep rate ($50 \text{ A m}^{-1} \text{ s}^{-1}$) and at room temperature. The measurements show several steps and plateaus which are reproducible in step size and position (see inset in figure 4) and could correspond to the reversal of individual dots in the array. Moreover, the number of steps corresponds well with the number of dots in the central area of the cross, as expected. MFM measurements, done after the detection of a step in the Hall voltage, show that this step indeed corresponds to the reversal of an individual magnetic dot. These measurements were repeated several times and indicate that each step in the Hall voltage corresponds to the reversal of the same individual dot for all measurements (figure 5). Therefore, the use of the AHE makes it possible to measure the switching field of different individual dots in a large array.

An important result is that different switching field values are obtained for the same dot from one measurement to another. This variation in switching field, observed for all dots, is thermally induced (illustrated in figure 6). At 0 K, individual dots always switch at the same applied magnetic field value H_s^0 which cancels the energy barrier separating the two stable state of their magnetization (figure 6(a)). At elevated temperatures, the thermal energy $k_B T$ becomes sufficient to overcome this energy barrier and the magnetization can be reversed for a

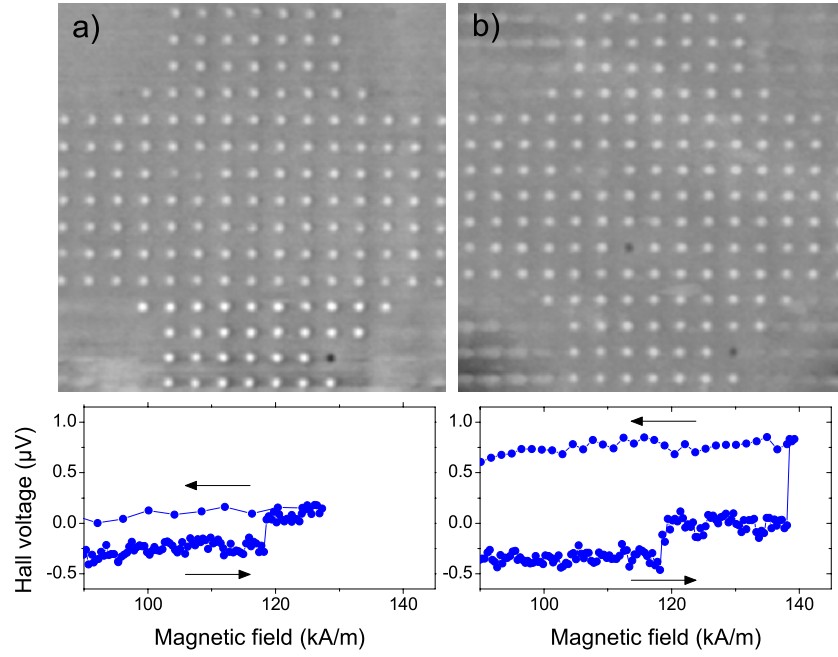


Figure 5. MFM images of a dot array measured after the detection of the first step (a) and the two first steps (b) in the Hall voltage. Upon detection of the first or second step, the magnetic field was ramped back to zero, after which the MFM measurement was performed. The steps in the Hall voltage always correspond to the reversal of the same dots. One can notice a bigger voltage step size for the switching of the second dot because the sensitivity is higher near the Hall cross center.

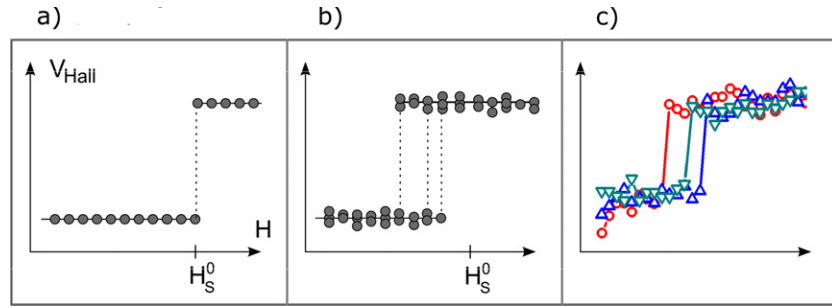


Figure 6. Sketches of several overlying curves showing the temperature effect on switching the field of one dot, and three experimental curves obtained for the first switching dot. (a) $T = 0$ K; (b) $T \gg 0$ K; (c) experimental.

magnetic field value lower than H_s^0 . Because of the thermal fluctuation, the switching field varies from measurement to measurement (figure 6(b)), which is in good agreement with the experimental observation (figure 6(c)). The SFD_T of individual dots was obtained from these measurements for comparison with the switching model.

4. Model for thermally induced switching field distributions

A straightforward Arrhenius-based model is used in order to calculate SFD_T . The model excludes the influence of neighboring dots due to stray field interactions, since we assume the reversal order of dots to be identical for every sweep. The stray field of neighboring dots is on the order of 1 kA m^{-1} [16], which is much smaller than the differences in switching fields for the first and last switching dots.

The probability $P_{sw}(\Delta t)$ that the magnetization of a dot has not switched after a time Δt is given by [2]:

$$P_{sw}(\Delta t) = \exp(-\Delta t/\tau(H, T)), \quad (3)$$

$$\tau(H, T) = f_0^{-1} \exp\left(\frac{E_b(H)}{k_B T}\right), \quad (4)$$

where f_0 is the attempt frequency (assumed to be close to 10^9 Hz [17]), E_b is the energy barrier, k_B is Boltzmann's constant and T the absolute temperature.

For the experiments, the applied magnetic field H is ramped with a rate R and the probability density $p_{sw}(H, T)$ that a switching occurs at a magnetic field H is given by [18]:

$$p_{sw}(H, T) = \frac{f_0}{R} \exp\left(\frac{-E_b(H)}{k_B T}\right) \times \exp\left[-\frac{f_0}{R} \int_0^H \exp\left(\frac{-E_b(h)}{k_B T}\right) dh\right]. \quad (5)$$

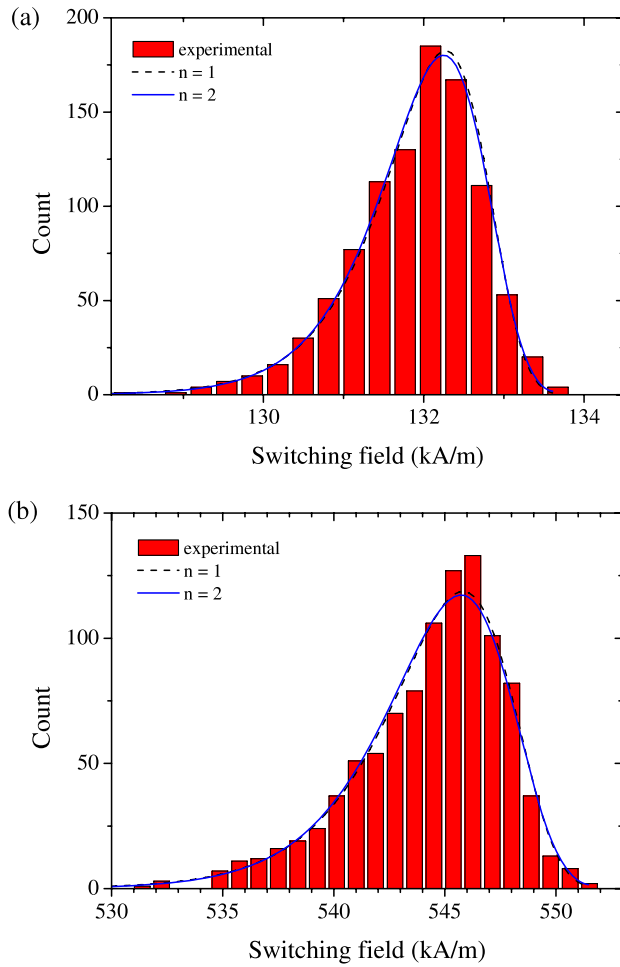


Figure 7. Histograms of 1000 measured switching fields H of the first weak dot and last strong dot. The lines are the probability density functions as obtained by fitting the model to the measurements. (a) The first weak dot. (b) The last strong dot.

This switching field distribution (SFD_T) can be estimated experimentally with the switching field histograms obtained by measuring the field value several hundred times for which a dot reverses its magnetization.

The energy barrier $E_b(H)$ is field dependent, and is commonly described by

$$E_b(H) = E_0 \left(1 - \frac{H}{H_s^0} \right)^n, \quad (6)$$

where E_0 is the energy barrier height without an externally applied field, and H_s^0 the switching field at $T = 0$ K [19]. The exponent n has an upper limit of 2 under conditions of pure coherent rotation (Stoner–Wohlfarth model), an external field aligned with the easy axis of magnetization and at 0 K. At elevated temperatures [20] or fields not aligned with the easy axis [21] the exponent is less than 2. The exponent n has a lower limit of 1 in the case of a thin film element which is much larger than the domain wall thickness, and in which the pinning of the domain wall is so weak that the wall does not bend under application of an external field [22]. For stronger pinning, the exponent is larger than 1.

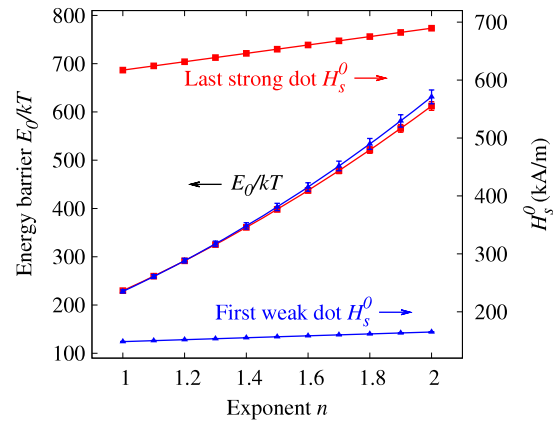


Figure 8. The values for E_0 and H_s^0 as a function of exponent n , obtained by fitting the model to the measured SFD_T. The curves for the energy barrier are almost identical, while the value of H_s^0 is larger for the last strong dot than for the first weak dot by more than a factor of 4.

Because we are measuring at room temperature and the dots under investigation are not perfect Stoner–Wohlfarth (SW) particles, and because there will be a distribution in easy axes from particle to particle, n is certainly lower than 2. On the other hand, since the dots are not large elements with weak pinning of domain walls (DW), n is certainly higher than 1. The calculation of the exact field dependence of the energy barrier requires numerical simulation [23] and is beyond the scope of this publication. Therefore we propose n to be a phenomenological parameter of which we only consider the extreme cases $n = 1$ (DW) and $n = 2$ (SW).

5. Switching field distribution of a single dot

Increasing field AHE measurements from negative saturation were repeated 1000 times at room temperature with $R = 50 \text{ A m}^{-1} \text{ s}^{-1}$. Some dots switch at low fields and others at relatively high fields; we call these ‘weak’ and ‘strong’ dots, respectively. Here we focus on the SFD_T of the first ‘weak’ dot (smallest switching field) and the last ‘strong’ dot (largest switching field) in order to determine the origin of the large difference between their average switching field value, 132 and 545 kA m^{-1} respectively. In figure 7, histograms of the measured SFD_T of both dots are shown, together with the results of fitting our model to the measurements for $n = 1$ and 2. The model’s distributions coincide well with the experimental SFD_T. Unfortunately, fits of equal quality can be found for every n between 1 and 2, thus it is impossible to directly infer the value of n from these measurements. Figure 8 shows the fit result values as a function of exponent n .

From E_0 and H_s^0 , the activation volumes for reversal can be calculated using $M_s = 1.2 \text{ MA m}^{-1}$ (table 1). For the domain wall propagation model ($n = 1$), the Barkhausen volume is [22]

$$V = \frac{E_0}{2\mu_0 M_s H_s^0}, \quad (7)$$

Table 1. The values for E_0 and H_s^0 from figure 8. The bottom rows show the switching volumes calculated from (7) and (8).

		Weak dot	Strong dot
$E_0/k_B T$	$n = 1$	228 ± 3	230 ± 2
	$n = 2$	631 ± 14	612 ± 9
H_s^0 (kA m ⁻¹)	$n = 1$	148.5 ± 0.3	617.2 ± 0.6
	$n = 2$	165.1 ± 0.5	689.5 ± 1.4
V	$n = 1$	$(13 \text{ nm})^3$	$(8 \text{ nm})^3$
	$n = 2$	$(28 \text{ nm})^3$	$(17 \text{ nm})^3$

whereas for the SW model ($n = 2$), the nucleation volume V and the effective anisotropy constant K are [24]

$$V = \frac{2E_0}{\mu_0 M_s H_s^0}, \quad K = \frac{\mu_0 M_s H_s^0}{2}. \quad (8)$$

6. Discussion

Within the framework of our simple model, the difference in switching fields between the weak and strong dot in our experiment is caused by a difference in the energy barriers. This difference can be caused by a difference in switching mechanism n , switching volume V , or switching field at 0 K H_s^0 . Since the SFD_T is equally well fitted by any value of n between 1 and 2, we cannot determine all three parameters. We can however discuss the two extreme cases $n = 1$ and 2.

If we assume that the dots reverse by the same switching mechanism (identical values of n), the energy barriers E_0 of the first and last switching dot are almost identical (figure 8). The difference in switching fields at room temperature is then caused by a difference in switching field at 0 K (H_s^0) by a factor of 4 (table 1). As a result, the switching volume of the weak dot is larger than that of the strong dot by a factor of about 4 as well.

On the other hand, if we assume that the switching volumes are almost identical, n for the weak dot has to be closer to 1, and n for the strong dot closer to 2, indicating a difference in reversal mechanism. Again, we must conclude that there is a difference in H_s^0 by at least a factor of 4.

The difference in H_s^0 can be caused by a difference in magnitude or direction of anisotropy. This anisotropy has various origins, both intrinsic to the material (crystal, stress) and caused by the shape of the elements. Previous studies on CoPt/Ru patterned films have shown that the SFD of dot arrays is well explained by a c -axis distribution [25], leading to a variation in the direction of intrinsic anisotropy, and therefore to a variation in the total effective anisotropy of the dots. We cannot fully exclude, however, that the variation can also be caused by other factors such as etch damage or redeposition during the etching of the dots.

The calculated switching volumes can be compared to physical parameters. From TEM observations the average grain diameter is found to be 14 nm [7]. With a film thickness of 20 nm, the average grain volume is $(15 \text{ nm})^3$, which is in excellent agreement with the calculated values in table 1.

The grains are however strongly exchange coupled, and the switching volume could extend over more grains. One

might argue therefore that the switching volume is not linked to the grain size, but proportional to the exchange length, or better the characteristic length l_c defined by Hubert [26, section 3.7.3c] in his analysis of domains in films with high perpendicular anisotropy:

$$l_c = \frac{\gamma_w}{2K_d} \quad (9a)$$

$$\gamma_w = 4\sqrt{AK_u} \quad (9b)$$

$$K_d = \frac{1}{2}\mu_0 M_s^2, \quad (9c)$$

where the wall energy γ_w can be calculated from the exchange constant $A = 9.5 \text{ pJ m}^{-1}$ [27] and the intrinsic anisotropy constant K_u . From the average intrinsic anisotropy of the film (1.3 MJ m^{-3}) we calculate the characteristic length to be 8 nm. This gives a minimum diameter for bubble domains of about 30 nm, which is on the order of the calculated values in table 1. So changes in grain size or critical length scale could both be at the origin of changes in the switching volume.

If we assume that changes in grain size are at the origin of the changes in switching volume, and we further assume that the grains extend through the complete film, the grain diameter varies from 5 to 10 nm for $n = 1$, and from 16 to 34 nm for $n = 2$. However, dots with the highest switching fields have the smallest grains, which seems unlikely.

We could assume on the other hand that changes in anisotropy cause changes in switching volume. For equal values of n , H_s^0 is 4.2 times larger for the last dot than for the first dot. Assuming that K_u is proportional to H_s^0 , the characteristic length l_c of the last dot equals more than two times the l_c of the first dot, which is in good agreement with the calculated values for the difference in switching volumes in table 1. It should be noted, however, that the energy barrier E_0 is not solely determined by the intrinsic anisotropy K_u , since during switching the external stray field energy will also be reduced. An exact calculation will require detailed micromagnetic knowledge on the reversal process, which surpasses the scope of this paper. Compensating for this effect, however, will always lead to larger calculated differences in switching volume.

Summarizing, it is plausible that the calculated differences in switching volume are caused by a difference in critical length scales, caused by a difference in effective anisotropy between the weak and strong dot.

Additional experiments are required to further unravel the origins for the variation in switching fields between dots. The AHE measurement method presented here provides a powerful tool. A comparison of the temperature dependence of the switching fields is planned for future work and will provide more information about the difference in reversal mechanisms between the dots, as the temperature dependence of the switching field increases with n .

7. Conclusion

Using the anomalous Hall effect, it was possible to measure the perpendicular magnetization of a dot array of about 80

dots with diameters of 180 nm with high signal to noise ratio. This enables field measurements with multiple passes with low drift. At low and high switching fields, switching of individual dots is clearly observed. Hall voltage and MFM measurements indicate that these dots switch in a fixed order and that the variation of the switching field of individual dots can be measured. This switching field distribution (SFD_T) of a single dot is caused by thermal activation, and provides information on the energy barrier height.

The SFD_T of single dots fits very well to an Arrhenius type model, with energy barrier E_0 , switching volume V and a phenomenological parameter n representing the reversal mechanism as input. The value of n lies between 1 and 2. When the reversal mechanism is similar to coherent reversal, the value of n is close to 2. For domain wall motion, the value of n decreases towards 1. Unfortunately, it is not possible to infer the value of n from the SFD_T, because parameter fits of equal quality can be found for every n between 1 and 2.

Two dots were investigated in more detail, a 'weak' dot switching at 132 kA m^{-1} and a 'strong' dot switching at 544 kA m^{-1} . Interpretation of the AHE measurements leads to two opposite scenarios explaining the difference in switching fields. Assuming that the reversal mechanisms of both dots are identical (same value of n), the difference in switching fields between the dots must be caused by the fact that the weak dot has a switching field at 0 K which is a factor of 4 lower than that of the strong dot. On the other hand, if we assume that the switching volumes are identical, the difference in switching fields must be caused by differences in reversal mechanism, where the strong dot tends more towards coherent rotation. In this case the weak dot has a switching field at 0 K which is at least a factor of 4 lower. The real situation will be between these opposites, but we must conclude from our simple model that there must be a difference in the magnitude of the effective anisotropy between the two dots. It is plausible that the calculated difference in switching volumes between the dots is caused by a change in magnetic characteristic length scale due to a difference in effective anisotropy, although we cannot completely rule out variations in crystal size.

References

- [1] Thomson T, Hu G and Terris B D 2006 *Phys. Rev. Lett.* **96** 257204
- [2] Wernsdorfer W, Bonet Orozco E, Hasselbach K, Benoit A, Barbara B, Demoncey N, Loiseau A, Pascard H and Maily D 1997 *Phys. Rev. Lett.* **78** 1791
- [3] Grundler D, Meier G, Broocks K B, Heyn Ch and Heitmann D 1999 *J. Appl. Phys.* **85** 6175–7
- [4] Schuh D, Biberger J, Bauer A, Breuer W and Weiss D 2001 *IEEE Trans. Magn.* **37** 2091–3
- [5] Kikuchi N, Okamoto S, Kitakami O, Shimada Y and Fukamichi K 2003 *Appl. Phys. Lett.* **82** 4313–5
- [6] Wirth S and Von Molnár S 2000 *Appl. Phys. Lett.* **76** 3283–5
- [7] Kikuchi N, Murillo R, Lodder J C, Mitsuzuka K and Shimatsu T 2005 *IEEE Trans. Magn.* **41** 3613–5
- [8] Kikuchi N, Murillo R and Lodder J C 2005 *J. Appl. Phys.* **97** 10J713
- [9] Shimatsu T, Sato H, Oikawa T, Inaba Y, Kitakami O, Okamoto S, Aoi H, Muraoka H and Nakamura Y 2004 *IEEE Trans. Magn.* **40** 2483–5
- [10] Luttge R, van Wolferen H A G M and Abelmann L 2007 *J. Vac. Sci. Technol. B* **25** 2476–80
- [11] Nagaosa N 2006 *J. Phys. Soc. Japan* **75** 0420011
- [12] Sinitsyn N A 2008 *J. Phys.: Condens. Matter* **20** 023201
- [13] Webb B C and Schultz S 1988 *IEEE Trans. Magn.* **24** 3006–8
- [14] Hu G, Thomson T, Rettner C T and Terris B D 2005 *IEEE Trans. Magn.* **41** 3589–91
- [15] Schumacher F 1991 *J. Appl. Phys.* **70** 3184
- [16] Murillo Vallejo R 2006 Magnetic media patterned by laser interference lithography *PhD Thesis* University of Twente Enschede, The Netherlands
- [17] Weller D and Moser A 1999 *IEEE Trans. Magn.* **35** 4423–39
- [18] Wang H T, Chui S T, Oriade A and Shi J 2004 *Phys. Rev. B* **69** 064417
- [19] Sharrock M P 1994 *J. Appl. Phys.* **76** 6413–8
- [20] Bennett L H, Della Torre E, DeWit R, Kahler G and Watson R E 2006 *J. Appl. Phys.* **99** 08K507
- [21] Victora R H 1989 *Phys. Rev. Lett.* **63** 457–60
- [22] Gaunt P 1986 *J. Appl. Phys.* **59** 4129–32
- [23] Brown W F 1963 *Phys. Rev.* **130** 1677–86
- [24] Sharrock M P and McKinney J T 1981 *IEEE Trans. Magn.* **17** 3020–2
- [25] Mitsuzuka K, Shimatsu T, Muraoka H, Kikuchi N and Lodder J C 2006 *J. Magn. Soc. Japan* **30** 100–7
- [26] Hubert A and Schäfer R 1998 *Magnetic Domains: The Analysis of Magnetic Microstructures* (Berlin: Springer)
- [27] Mitsuzuka K, Kikuchi N, Shimatsu T, Kitakami O, Aoi H, Muraoka H and Lodder J C 2006 *IEEE Trans. Magn.* **42** 3883–5